




Cite this: *Sens. Diagn.*, 2024, **3**, 1442

## Stretchable and body-conformable physical sensors for emerging wearable technology

Yong Lin, Weijie Qiu and Desheng Kong \*

Wearable physical sensors represent attractive devices for health monitoring and human-machine interfaces. Unlike traditional devices that prioritize increased sensitivity and selectivity, stretchability is crucial for wearable sensors to effectively adhere to the dynamic and curved contours of the human body. In addition to being stretchable, the conformal integration allows for durable skin-device interfaces, enabling long-term wearable detection. To track the latest progress, this perspective focuses on the rapidly advancing field of skin-attached physical sensors, analyzing their design approaches, critical applications, and desirable characteristics. The discussion begins with two primary strategies for creating stretchable electronic devices through structural designs and material innovations. We further discuss the significance of a conformal, seamless skin-device interface for wearable detection. We further elaborate on several critical physical sensors and their system integration. Finally, this article addresses current challenges and outlines future directions to translate knowledge in this evolving field into cutting-edge wearable technologies.

Received 5th June 2024,  
Accepted 24th July 2024

DOI: 10.1039/d4sd00189c

[rsc.li/sensors](https://rsc.li/sensors)

## 1. Introduction

The field of stretchable electronics has witnessed substantial advancements in recent years, attributed to progress in material science, device design, and processing techniques.<sup>1–3</sup> These emerging devices hold significant potential across various sectors, including health monitoring, human-machine interfaces, and advanced prosthetics.<sup>4–7</sup> Stretchable sensors play a crucial role in converting physical, chemical, or biological signals from the body into valuable data for assessing an individual's health.<sup>8–11</sup> The seamless integration of these devices with the human body is essential, ensuring a mechanically stable interface for reliable long-term detection. Compliant physical sensors are particularly attractive for executing continuous and real-time measurements on the skin, effectively probing physiological processes and micromotions.<sup>12,13</sup> In addition to the requirement of mechanical deformability and skin conformability, these sensors should also pursue sensitivity, selectivity, and response speed for accurate and reliable measurements in wearable settings.<sup>14</sup>

The skin is a soft organ that can undergo significant deformation up to 60% strain during joint movements.<sup>15</sup> However, conventional electronic materials are rigid and can only withstand minimal strain before failing.<sup>6,16</sup> The

mechanical disparity between biological tissues and engineering materials makes it difficult for functional devices to operate reliably on the skin. To address these challenges, flexible and stretchable electronics have been developed for the next generation of wearable technology. Stretchable materials and structures allow sensors to take on highly deformable forms, which is important for following the curvilinear and dynamic contours of the human body.<sup>17,18</sup> Given the three-dimensional curvatures of body parts, electronic devices must be able to bend and stretch to conform to these intricate geometries.<sup>19</sup> As discussed in several reviews, stretchability is considered a crucial requirement for devices to achieve body integration on a macroscale level.<sup>6,12,20–22</sup> On the other hand, the uneven surface of the skin, characterized by wrinkles and ridges, presents challenges for the devices to establish intimate interfaces without air gaps.<sup>15,23</sup> Besides being stretchable, these devices also require a thin form to minimize bending stiffness. A microscopic conformal interface can significantly increase the contact areas with the skin, thereby enhancing the sensing signals.<sup>24–26</sup> Consequently, both stretchability and conformability are essential attributes for physical sensors to achieve reliable detection when affixed to the body.

This perspective presents an overview of recent advancements and potential applications of stretchable and body-conformable physical sensors as an emerging wearable technology. Firstly, we discuss the techniques for developing stretchable electronic devices through structural designs and

College of Engineering and Applied Sciences, State Key Laboratory of Analytical Chemistry for Life Science, and Jiangsu Key Laboratory of Artificial Functional Materials, Nanjing University, Nanjing 210023, China. E-mail: [dskong@nju.edu.cn](mailto:dskong@nju.edu.cn)



material innovations. We then emphasize the significance of body conformability in sensing devices for wearable detection. Next, we outline various types of wearable physical sensors and their integrated systems for monitoring different signals, such as biopotential, hydration, temperature, and pressure. Additionally, we elaborate on the desired attributes of these sensors, such as adhesion, biocompatibility, and permeability. Our goal is to encourage the exploration of new materials and device designs for the next generation of wearable physical sensors.

## 2. Methodology and approach

This perspective presents a comprehensive overview of this active area through a semi-systematic assessment. The literature review of recent research activities commences by conducting a search for pertinent publications using Google Scholar based on combined keywords, such as stretchable, body-conformable, and physical sensors. In the appraisal stage, inclusion criteria were applied, with a focus on recent publications, specifically within the last decade. The chosen publications explicitly discuss stretchable electronic devices or wearable physical sensors. The synthesis stage encompasses two crucial tasks: the extraction and categorization of publications, followed by the subsequent synthesis of insights and conclusions. Lastly, the findings were critically analyzed to identify significant challenges.

## 3. Stretchable electronic devices

Stretchable electronics is an emerging technology that has experienced rapid advancement in the past decade. Unlike conventional electronic technology focusing on enhanced processing speed and energy efficiency, stretchable electronics prioritize mechanical flexibility and structural deformability. These devices can endure repetitive bending, twisting, and stretching without experiencing degradation in their properties. Currently, there are two primary approaches for creating stretchable electronic devices, including structural designs and material developments.

### 3.1 Structural designs

Structural designs make use of a wide range of traditional optoelectronic materials. They harness specifically tailored structures to manipulate strain distribution, achieving stretchability at the device or system levels. By adopting buckled,<sup>27</sup> serpentine,<sup>28</sup> kirigami,<sup>29</sup> and wavy structures,<sup>30</sup> non-extensible materials can be morphed into stretchable forms with minimal compromise to their performance characteristics. These structures provide internal space in stretchable devices, allowing for expansion during stretching with minimal strains in the materials. One effective method involves patterning the functional materials into an in-plane filamentary network of serpentine structures, where the device's upper limit of stretchability is controlled by the

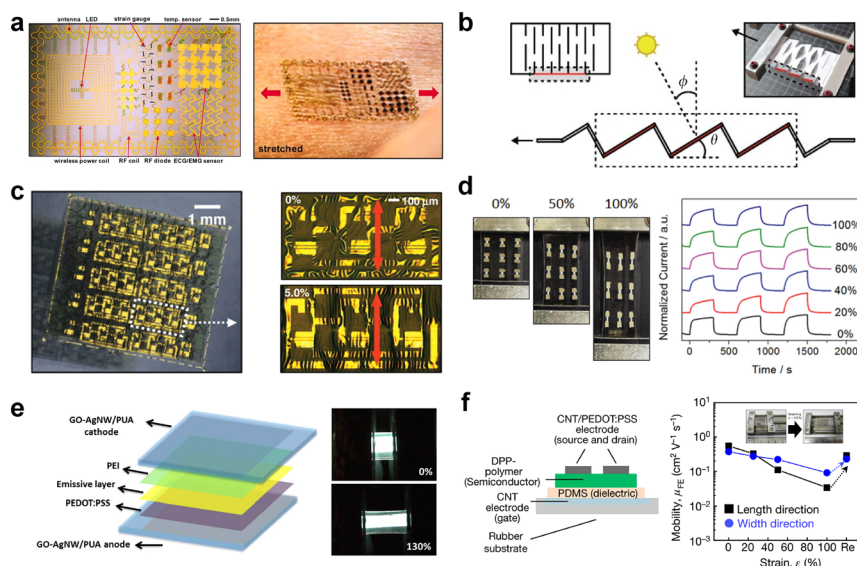


**Fig. 1** a) Multifunctional electronic devices harnessing filamentary serpentine structures to achieve mechanical stretchability. Reproduced with permission from ref. 28. Copyright 2011 The American Association for the Advancement of Science. b) Schematic design and optical image of a thin-film solar cell with kirigami cuts for dynamic sunlight tracking. Reproduced with permission from ref. 29. Copyright 2015 Springer Nature. c) Optical images of a biaxial stretchable integrated circuit using out-of-plane, wavy designs. Reproduced with permission from ref. 30. Copyright 2008 The American Association for the Advancement of Science. d) Intrinsically stretchable photodetectors composed of ZnO NW channels and Ag NW electrodes on a polydimethylsiloxane (PDMS) substrate. Reproduced with permission from ref. 31. Copyright 2014 John Wiley and Sons. e) Intrinsically stretchable organic light-emitting diodes based on nanocomposite electrodes and polymer emissive layers that can withstand up to 130% strain. Reproduced with permission from ref. 32. Copyright 2014 American Chemical Society. f) Intrinsically stretchable organic thin-film transistors based on nanocomposite electrodes and polymer semiconductors. Reproduced with permission from ref. 33. Copyright 2016 Springer Nature.



wavelength and magnitude of the curvy structures (Fig. 1a).<sup>28</sup> Furthermore, the kirigami strategy enables stretchability by introducing periodic cutting patterns. The cuts dissipate applied loads to mitigate stress concentrations around the active areas. For example, a solar cell with a dynamic tracking response system based on a buckled kirigami structure has been introduced,<sup>29</sup> as shown in Fig. 1b. Compared to conventional solar tracking systems with complex mechanical components, the kirigami structure achieves large deformability in a simplified actuation scheme, significantly reducing weight and cost. Another approach employs out-of-plane, wavy designs, where tensile strains are mainly absorbed by flattening these structures under strain. As shown in Fig. 1c, stretchable integrated circuits with biaxial stretchability were realized using 2D wavy structures, enabling reliable operation despite external stretching in any direction within the circuit's plane.<sup>30</sup>

In summary, the research on deformable structures presents a robust and versatile strategy for imparting stretchability to existing electronic materials and devices. These efforts allow state-of-the-art optoelectronic materials to be used in these emerging areas. However, the fabrication of intricate strain relief microstructures often necessitates complex fabrication processes and advanced facilities. Numerical simulations are often necessary for achieving the optimal design of highly stretchable structures. Additionally, the deformable microstructures in these devices take up extra space, either horizontally or vertically, which presents challenges for device miniaturization and high-density integration.

### 3.2 Material innovations

An alternative strategy harnesses all compliant material components to create functional devices with mechanical stretchability. Such devices are referred to as intrinsically stretchable devices, in contrast to those that require structural engineering. These materials have the inherent ability to deform and accommodate significant strains. To successfully fabricate these devices, it is essential to develop a whole range of compliant building materials, encompassing conductors, semiconductors, and insulators/dielectrics. Stretchable conductors are used to construct functional electrodes and electrical interconnects in devices. One widely studied material system for this purpose is conductive nanocomposites, formed by dispersing various nanostructures into elastomers. The commonly used nanostructures include metal nanoparticles,<sup>34</sup> metal nanowires,<sup>32,35,36</sup> and metal nanoflakes.<sup>37–39</sup> These nanocomposites have a three-dimensional percolation network of conductive nanofillers, allowing for excellent electrical conductivity and mechanical deformability. Additionally, conducting polymers, such as polyaniline (PANI) and poly(3,4-ethylenedioxythiophene):polystyrene sulfonate (PEDOT:PSS), are used due to their combined charge transport and mechanical flexibility.<sup>40</sup> Soft and

biocompatible hydrogels with high water contents are also popular choices for ionically conductive materials.<sup>41,42</sup> Gallium-based liquid metal (LM) alloys, which remain molten at room temperature, are an emerging class of electronic conductors characterized by high electrical/thermal conductivity and liquid-phase flowability.<sup>43–45</sup> Stretchable semiconductors are typically synthesized from  $\pi$ -conjugated polymers and small molecules with the inherent advantages of mechanical deformability. Their electrical and mechanical properties can be adjusted by controlling the molecular structures through synthesis. An alternative approach involves blending conjugated polymers with soft elastomers to create stretchable semiconductors.<sup>46,47</sup> Stretchable insulators are crucial for constructing dielectric layers, substrates, or encapsulation layers of functional devices. A variety of elastomers are used for this purpose, including poly(dimethylsiloxane) (PDMS), polyurethane (PU), Ecoflex, and butadiene copolymer. The dielectric constants of these materials are directly affected by the polarizability of their molecular structures. For example, PDMS, styrene-butylene-styrene (SBS), and styrene-isoprene-styrene (SIS) elastomers exhibit a low dielectric constant of 2 to 3, whereas poly(vinylidene fluoride) (PVDF)-based block copolymers display a high dielectric constant above 10.<sup>48</sup> Modifications have been made through blended elastomer and ceramic nanoparticle composites, resulting in a significant increase in the dielectric constant by several folds.<sup>49,50</sup>

The development of intrinsically stretchable electronic devices has been a significant focus in recent years. Lee *et al.* developed a stretchable photodetector for optoelectronic applications using silver nanowire (Ag NW) electrodes and zinc oxide NW channels.<sup>31</sup> These nanocomposite materials were patterned and embedded into a PDMS substrate, as shown in Fig. 1d. Three photodetectors in series showed stable on/off behavior even under mechanical distortions. Additionally, Liang *et al.* embedded Ag NWs and graphene oxides into polyurethane acrylate (PUA) substrates to create transparent and stretchable electrodes.<sup>32</sup> They positioned an emissive polymer layer between two transparent electrodes to construct an organic light-emitting diode, as depicted in Fig. 1e, utilizing PEDOT:PSS and polyethyleneimine as charge transporting layers. The resulting device has skin-like stretchability and can endure up to 130% strain. Furthermore, Bao *et al.* reported stretchable organic thin-film transistors based on semiconducting polymers.<sup>33</sup> The mobility gradually decreased upon stretching up to 100% strain but could mostly be recovered to their initial values after releasing the strain (see Fig. 1f).

Significant progress has been made in developing stretchable electronic materials, but controlled fabrication remains a major bottleneck for device development. Currently, most intrinsically stretchable materials are prepared through solution processes, posing challenges for multi-layer stacked devices. The potential fabrication issues involve dissolution, mixing, or cracking of the underlying layers. The design and fabrication of advanced devices based



on intrinsically stretchable components are still vital direction for future research.

## 4. Body-conformable electronic device

The body comprises soft biological tissues that can undergo significant structural deformations. Stretchability is crucial for sensing devices to follow the body's dynamic contours. However, the ability to stretch does not automatically ensure that the devices can conform to the body. All body parts exhibit three-dimensional surfaces characterized by global curvatures, while at the microscale, the skin presents a rough surface with wrinkles that define local curvatures. These curvatures determine the level of bending and stretching required for sensors to wrap around the body. Most devices constructed on elastomer substrates can generally conform to the global curvature of body parts, providing a basic level of body conformability necessary for long-term secure integration. Body-mounted devices provide an appealing platform for integrating various electronic functionality. These devices have advanced beyond simple sensing to include actuation like drug delivery<sup>51</sup> and electrical stimulation.<sup>52</sup> Over the past few years, we have witnessed exciting developments in this area. Progress in optoelectronic materials and fabrication techniques has enabled display devices suitable for seamless integration with the body.<sup>53</sup> Some emerging strain sensors can provide a mechanical sensation when attached to textured skin surfaces.<sup>54</sup> Notably, a significant breakthrough has been achieved by developing body-conformable ultrasonic imagers for internal organs.<sup>55</sup> Additionally, a chipless surface acoustic wave sensor array has been demonstrated to monitor glucose concentrations, blood pressure, heart rate, and activities.<sup>56</sup> As new materials and properties emerge, the range of applications uniquely achievable with body-conformable electronic devices continues to expand. However, achieving full conformity to the microscale curvature of the skin is exceedingly difficult. Eliminating air gaps at the skin-device interfaces requires a considerable stiffness reduction in the sensors (Fig. 2). This full surface coverage can help the sensors maximize their responsivity (Fig. 2). Unfortunately, ideal body conformability has been only achieved in very limited systems, such as ultrathin elastomers, soft hydrogels, and liquid materials.

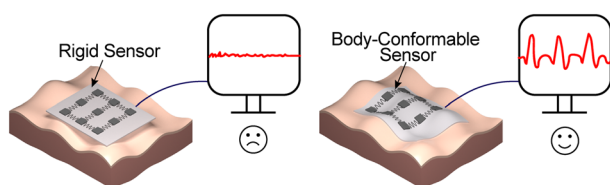


**Fig. 2** Schematic illustrating different modes of interaction with textured skin surfaces for a rigid sensor (left) and a body-conformable sensor (right).

The ability to conform to the body represents a critical design consideration for next-generation wearable sensors.

## 5. Physical sensors

The significance of on-body sensing cannot be overstated in fundamental research, clinical diagnostics, and personalized medical devices. Stretchable physical sensors play a crucial role in establishing a seamless and conformable interface between electronics and biological systems, facilitating the continuous collection of precise signals. A typical sensor works by converting physiological characteristics into an electronic response through various transduction mechanisms, which may involve changes in capacitance, resistance, current, and voltage. Fig. 3 shows the increasing use of physical sensors to detect various signals, such as biopotential, hydration, temperature, and pressure. Furthermore, integrating physical sensors with other functional modules, including data processing, power sources, and wireless communication, is essential for developing standalone wearable systems suitable for practical applications (Fig. 3).

### 5.1 Biopotential sensor

Cells produce bioelectricity through ion channels in their membranes, leading to detectable biopotentials in the human body. These low-level electrical potentials encompass electrocardiogram (ECG), electromyogram (EMG), electrooculogram (EOG), and electroencephalogram (EEG).<sup>57,58</sup> Biopotential sensors are typically affixed to the skin to capture these signals as distinct waveforms. Extensive research has been dedicated to acquiring signals with a high signal-to-noise ratio (SNR), forming the foundation for identifying abnormal features as indicators of health issues. The reliable capture of biopotential signals relies on the secure placement of biopotential sensors on the skin. When designing biopotential sensors, it is essential to consider the SNR that hinges on contact impedance. Lowering the contact

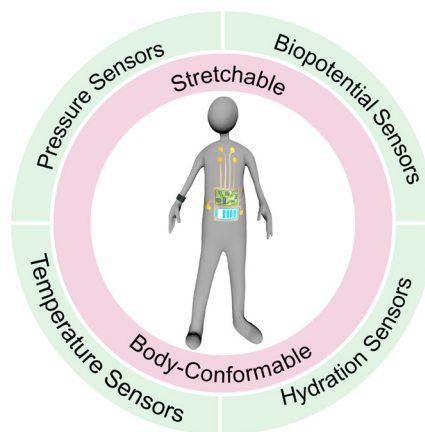


**Fig. 3** Stretchable and body-conformable physical sensors to enable sustained wearable detection without interrupting daily activities.





impedance leads to improved signal quality and increased SNRs. For instance, the liquid metal micromesh electrodes have lower skin-electrode contact impedance than commercial Ag/AgCl gel electrodes due to their compliant mechanical properties and high conductivity.<sup>59</sup> The conformal coverage on the textured skin surface helps maximize the contact area for optimal signal recording.<sup>60,61</sup> As a result, the SNR of EMG waveforms is slightly higher using liquid metal micromesh electrodes.<sup>59</sup> In practice, poor contact can lead to random impedance changes and triboelectric charges when the skin is deformed. It is essential to secure these biopotential sensors on the skin. For example, soft hydrogel sensors have low modulus and strong tissue affinity, which can effectively cut down motion-induced artefacts.<sup>42</sup>

ECG signals are considered pivotal for assessing cardiovascular health.<sup>62–64</sup> Ding *et al.* introduced a skin-adhesive liquid metal particle (ALMP) formed by *in situ* deposition (Fig. 4a).<sup>63</sup> The electrodes exhibit low contact impedance owing to their conformability and self-

adhesiveness to the skin (Fig. 4a). The ECG waveforms captured by ALMP sensor are very clear with significantly reduced noises (Fig. 4a).

EMG signals correspond to the muscular activity present in the human body and can be leveraged to diagnose muscle-related disorders.<sup>69</sup> For instance, Parkinson disease (PD) is a condition characterized by the degeneration of dopaminergic neurons in the brain, leading to an imbalance in dopamine production and subsequent motor disturbances.<sup>70</sup> The resulting motoric disorders manifest as distinct electrical signals detectable by EMG. Several methods have been developed to use EMG as a diagnostic tool for PD-related motoric symptoms, such as rigidity, gait abnormality, and tremor.<sup>71</sup> Moreover, abnormal EMG signals detected in the chin region may have potential links to head and neck cancer, leading to difficulties in swallowing. In terms of fabrication, an electronic tattoo form of EMG sensors has been created using laser-induced hierarchical carbon nanofibers (LIHCNFs),<sup>65</sup> as shown in Fig. 4b. Upon mounting on the forearm, this sensor effectively captured EMG signals

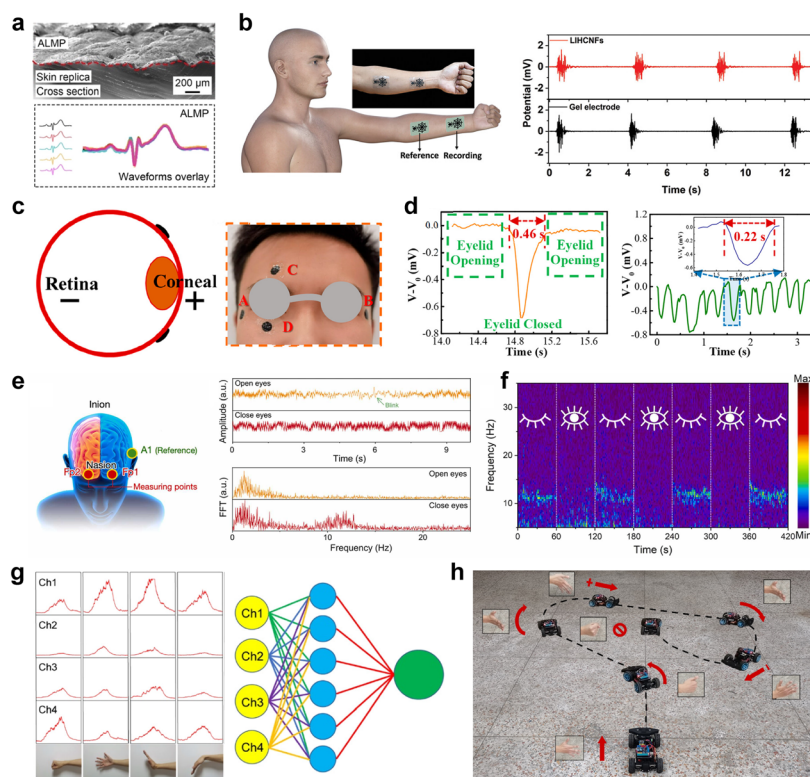


**Fig. 4** a) SEM images of skin-adhesive liquid metal particles (ALMPs) attached to the skin replica (top) and corresponding multiple detected ECG waveforms overlapped to demonstrate the detection stability (bottom). Reproduced with permission from ref. 63. Copyright 2022 American Chemical Society. b) Acquisition of EMG signals by laser-induced hierarchical carbon nanofibre (LIHCNF) tattoo sensors and commercial gel electrodes. Reproduced with permission from ref. 65. Copyright 2021 John Wiley and Sons. c) Graphene-based sensors attached around the eye for EOG testing. d) EOG waveform during a single normal blinking (left) and continuous fast blinking (right). The inset shows the waveform of a single blink cycle. e and f) Reproduced with permission from ref. 66. Copyright 2022 American Chemical Society. e) EEG signals and corresponding fast Fourier transform-processed frequency distributions in eye-closed and open states. f) Time-frequency spectrogram of the EEG signals during eye closing/opening cycles, revealing the dynamic activity of the alpha rhythm at  $\approx 10$  Hz. e and f) Reproduced with permission from ref. 67. Copyright 2023 Elsevier. g) Acquired multichannel EMG signals analyzed by a machine learning algorithm into corresponding hand gestures, thereby enabling a smart human-machine interface. h) Controlling a four-wheel car wirelessly by hand gesture commands. g and h) Reproduced with permission from ref. 68. Copyright 2021 American Chemical Society.



associated with muscle contractions, demonstrating comparable performance to that of commercial gel electrodes.

EOG signals are closely related to vergence eye motions. Xu *et al.* developed a thin and permeable EOG sensor created by transferring laser-induced honeycomb graphene onto a PU tape.<sup>66</sup> When placed at the corner of the eye, the sensor accurately detected the duration of eyelid opening and closing, as demonstrated in Fig. 4c, with a period of 0.46 seconds for a single eye-blink cycle (Fig. 4d). Fig. 4d also illustrates that the sensor effectively monitored eye-blink signals when the subject blinked at twice the normal rate (2.2 Hz  $\rightarrow$  4.5 Hz). Changes in the brain's short-term activity affect the frequency of eye blinking, making it possible to utilize the sensor to distinguish between normal blinking, sleepiness, and dry eyes (Fig. 4d).

EEG signals from brain activities provide valuable insights into neurological disorders and human emotions.<sup>72</sup> Dong *et al.* have introduced a method to create highly ultrastretchable and conductive electronic textiles as on-skin

sensors, involving a pre-stretching activation strategy of liquid metal deposited on the textile.<sup>67</sup> The textile sensor can acquire high-fidelity EEG signals, as depicted in Fig. 4e. When a subject is relaxed with their eyes closed, the EEG background typically displays the posteriorly dominant  $\alpha$  rhythm, characterized by a prominent oscillation of 8–12 Hz (Fig. 4e). This pattern aligns with brain activities associated with meditation and mindfulness, which are known to reduce stress levels. The  $\alpha$  rhythm notably diminishes when the eyes are open, demonstrating the dynamic nature of the  $\alpha$  rhythm during repeated eye-closing and eye-opening (Fig. 4f).

The analysis of biopotential signals can be utilized to interpret human intention for emerging applications in human-machine interfaces (HMIs).<sup>68,73,74</sup> Numerous studies have highlighted the suitability of on-skin sensors in acquiring high-quality biopotential signals. For instance, Zhao *et al.* developed a sophisticated epidermal HMI as a smart arm sleeve to capture control commands based on hand gestures.<sup>68</sup> As depicted in Fig. 4g, the sensors

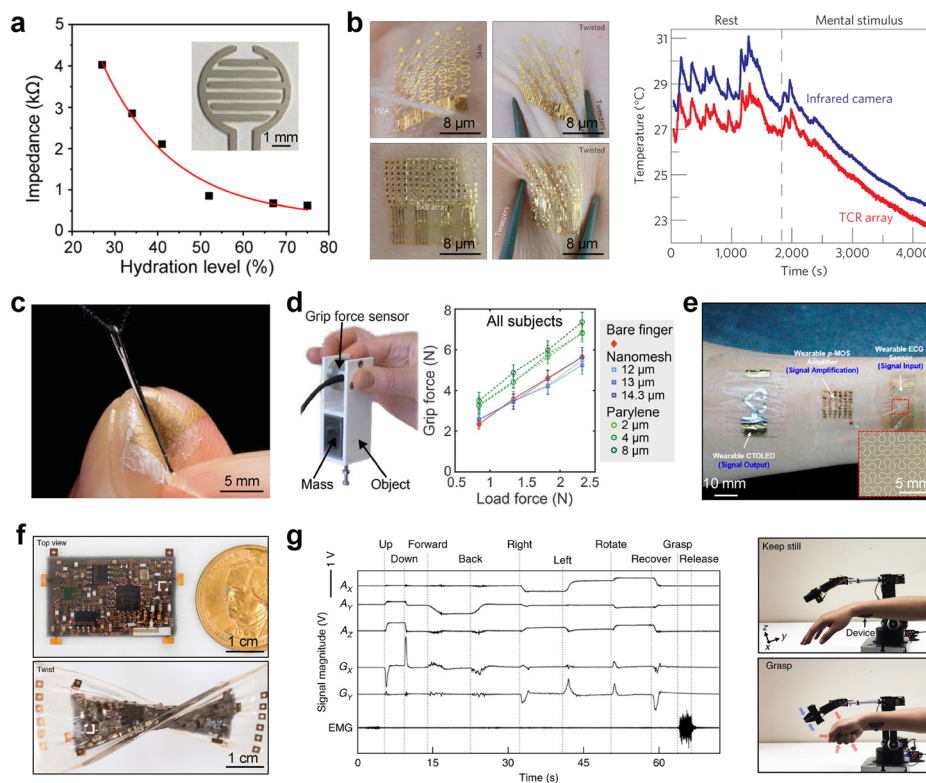


**Fig. 5** a) Measured impedance of a hydration sensor with respect to the skin hydration level. Inset: Optical image of the hydration sensor based on Ag NW nanocomposite electrodes attached to the skin. Reproduced with permission from ref. 75. Copyright 2023 American Chemical Society. b) Stretchable resistance temperature detectors based on Au thin film with conformal attachment to the skin, revealing the temperature of the palm measured with an infrared camera (blue) and a sensor array (red, offset for clarity) during mental stimulus tests. Reproduced with permission from ref. 77. Copyright 2013 Springer Nature. c) Optical image showing a nanomesh pressure sensor conformally attached to an index finger. d) Influence of nanomesh and parylene pressure sensors on the grip force to lift varying loads. c and d) Reproduced with permission from ref. 78. Copyright 2020 The American Association for the Advancement of Science. e) Wearable sensing system consisting of ECG sensors, a carbon nanotube (CNT)-based amplifier, and a color-tunable organic light emitting diode. The inset is a magnified view of the ECG sensor. Reproduced with permission from ref. 79. Copyright 2017 American Chemical Society. f) Optical image showing of a three-dimensional integrated electronic system using chip-scale components under relaxed (top) and twisted (bottom) conditions. g) Simultaneously acquired acceleration ( $A_x$ ,  $A_y$ , and  $A_z$ ), angular velocity ( $G_x$  and  $G_y$ ), and EMG data using the integrated sensing system to control a robotic arm. f and g) Reproduced with permission from ref. 80. Copyright 2018 Springer Nature.

embedded in the arm sleeve capture the EMG signals from several key muscles on the forearms. The gestures are related to distinctive EMG waveforms in these sensor channels due to the coordinated contractions of muscle groups (Fig. 4g). The machine learning algorithm helps decipher these waveforms as gesture commands, thereby establishing advanced HMIs (Fig. 4h).

### 5.2 Hydration sensor

The hydration level of the skin is a key metric for assessing skin quality and overall health. Skin hydration is commonly evaluated through impedance measurements, where an increase in hydration level leads to enhanced ionic conductivity and decreased impedance value.<sup>59,75</sup> These measurements are typically conducted at a relatively high frequency, in the order of  $10^2$  kHz, to minimize the impact of skin-electrode contacts. A common measurement approach utilizes compliant sensors in the form of interdigitated electrodes attached to the skin,<sup>75</sup> as depicted in Fig. 5a. These devices not only provide stable skin hydration readings in indoor settings but also enable the monitoring of dynamic changes following the application of moisturizers. In another study, Huang *et al.* described a hydration monitor that uses an array of impedance sensors to map the distribution of skin hydration levels.<sup>76</sup> Expanding the spacing between the sensors allows for increased measurement depth, enabling partial measurement of hydration levels below the stratum corneum. The device can quantify regional hydration information to shed light on skin health.

### 5.3 Temperature sensors

The human body maintains its temperature through the interplay of heat generation and dissipation. Body temperature is a crucial indicator for assessing activity levels and overall health. An abnormal rise in body temperature may indicate inflammation or fever, making it a valuable auxiliary diagnostic tool for various conditions such as cardiovascular disease and cancer.<sup>81</sup> Stretchable sensors that conform to the skin are essential for measuring temperature using different mechanisms, including resistance temperature detectors (RTDs),<sup>82</sup> thermistors,<sup>83</sup> pyroelectric,<sup>84</sup> and thermoelectric sensors.<sup>85</sup> RTDs are commonly used for converting temperature to resistance changes due to their high linearity, broad working range, and stability. Accurate and continuous thermal characterization of the human body necessitates the development of ultrathin, conformal, and stretchable RTDs,<sup>77</sup> as depicted in Fig. 5b. Continuous temperature monitoring on the forearm during a 60-minute rest period demonstrates advanced monitoring capabilities beyond conventional rigid probes, revealing minor fluctuations in skin temperatures associated with periodic contraction and dilation of the vessel (vasomotion). The temperature coefficient of resistance (TCR) is a crucial parameter in assessing the sensitivity of RTDs. It is defined by the equation  $TCR = (1/R_0) \cdot (\Delta R / \Delta T)$ , where  $\Delta R$  denotes the

change in resistance,  $R_0$  represents the original resistance, and  $\Delta T$  indicates the change in temperature. When utilizing RTDs in practical settings, it is crucial to consider both the measurement range and the TCR. For example, Yang *et al.* showcased an ultrasensitive device based on graphene nanowalls and PDMS, featuring a measurement range of 25–100 °C and a TCR of  $0.214\% \text{ } ^\circ\text{C}^{-1}$ .<sup>86</sup> Furthermore, Bae *et al.* created a flexible temperature sensor by spray coating rGO on a parylene C substrate, demonstrating a constant TCR of  $0.83\% \text{ } ^\circ\text{C}^{-1}$  within 22–70 °C and a rapid response to temperature changes within 100 ms.<sup>87</sup> Additionally, Zhu *et al.* introduced circuit design strategies to improve the robustness and accuracy of a CNT-based flexible temperature sensor with a high TCR of  $1.435\% \text{ } ^\circ\text{C}^{-1}$ .<sup>88</sup>

### 5.4 Pressure sensors

Pressure sensors can detect tactile information upon physical contact, making them invaluable for monitoring body movements and physiological activities such as pulse, breath, and heartbeat. Flexible pressure sensors primarily utilize piezoresistive and piezocapacitive mechanisms. Capacitive pressure sensors are commonly constructed using a parallel-plate capacitor architecture. The change in electrode distance or effective dielectric constant in response to applied pressure leads to capacitance variations. To enhance their sensitivity, various structural designs have been implemented, such as pyramids,<sup>89</sup> micropillars,<sup>90</sup> microdomes,<sup>91</sup> and wrinkles.<sup>92</sup> These designs enhance the responses by increasing geometric or contact variations under subtle external pressures. On the other hand, piezoresistive pressure sensors function by detecting changes in resistance when subjected to external pressure. The variation comes from two primary sources: either contact resistance or conductive layer resistance. Noteworthy features of piezoresistive sensors include a wide sensing range, simple device structure, extended operational lifespan, and ease of manufacturing. For instance, Luo *et al.* have developed a sensor using a piezoresistive material of carbon-black-decorated fabric and gold interdigital electrodes for cuffless blood pressure measurements.<sup>93</sup> Application of pressure results in a change in contact resistance, achieving a linear sensing range of 0–35 kPa and a sensitivity of  $0.585 \text{ kPa}^{-1}$ .<sup>93</sup> Similarly, Xu *et al.* created a resistive pressure-sensing device using laser-engraved silver-coated fabric, which exhibited a high sensitivity of  $6.417 \text{ kPa}^{-1}$  and a pressure sensing range of 0–800 kPa.<sup>94</sup> In addition to optimizing device designs, enhanced performance can be achieved through electronic systems. For example, Schwartz *et al.* introduced a pressure sensor coupled with transistors for amplification.<sup>95</sup> The resulting device can detect small features in the diastolic tail of the pulse pressure wave that most sensors used in arterial tonometry cannot detect. In next-generation prostheses, pressure-sensitive electronics can potentially restore amputees' sensory functions by interconnecting with nerve systems. Pressure sensors should possess not only high





sensitivity but also soft and thin form factors to minimize user disturbance. A recent study introduced an ultrathin nanomesh pressure sensor that can be attached to the skin with negligible impact on sensation,<sup>78</sup> as shown in Fig. 5c, evidenced by the lack of change in the grip forces required to hold weight. In contrast, a similar sensor on a 2  $\mu\text{m}$ -thick polymer film demands a 14% increase in grip force (Fig. 5d).

## 6. Integrated sensing systems

Integration of on-skin physical sensors with various functional modules such as data processing, power sources, and wireless communication modules is crucial in practical applications. This section discusses design and fabrication strategies for standalone on-skin sensor systems with multifunctionality. Proper integration strategies are essential for constructing flexible and stretchable sensing systems based on functional electronic components. A direct integration approach utilizes ultrathin elastomer membranes to construct a stretchable sensing system. Various compliant conductors, such as conductive tapes, metal wires, conductive paste/solders, and nanocomposites, are employed

to connect electronic components with mechanical deformability. A representative integrated system in thin-film forms comprises stretchable ECG sensors, inverter-based amplifiers, and a color-tunable organic light-emitting diode (LED),<sup>79</sup> as depicted in Fig. 5e. Initially, ECG signals are captured by ultrathin sensors on the skin, followed by amplification using a pseudo-complementary metal oxide semiconductor (CMOS) inverter. The processed signals with external computers are visualized by modulating the color of the LED using varying drive voltages, reflecting the cardiac health condition.

An alternative design employs vertical integration strategies to increase device density. Xu and colleagues recently introduced a three-dimensional integration to expand the functionality of stretchable sensing systems.<sup>80</sup> Compliant circuit layers with chip-scale components are aligned and vertically stacked in a layerwise sequence using transfer printing techniques, as illustrated in Fig. 5f. The resulting high-density integrated system exhibits deformable forms to withstand stretching, bending, twisting, and poking. Upon integration with different sensors to measure acceleration, angular velocity, and electromyography signals,

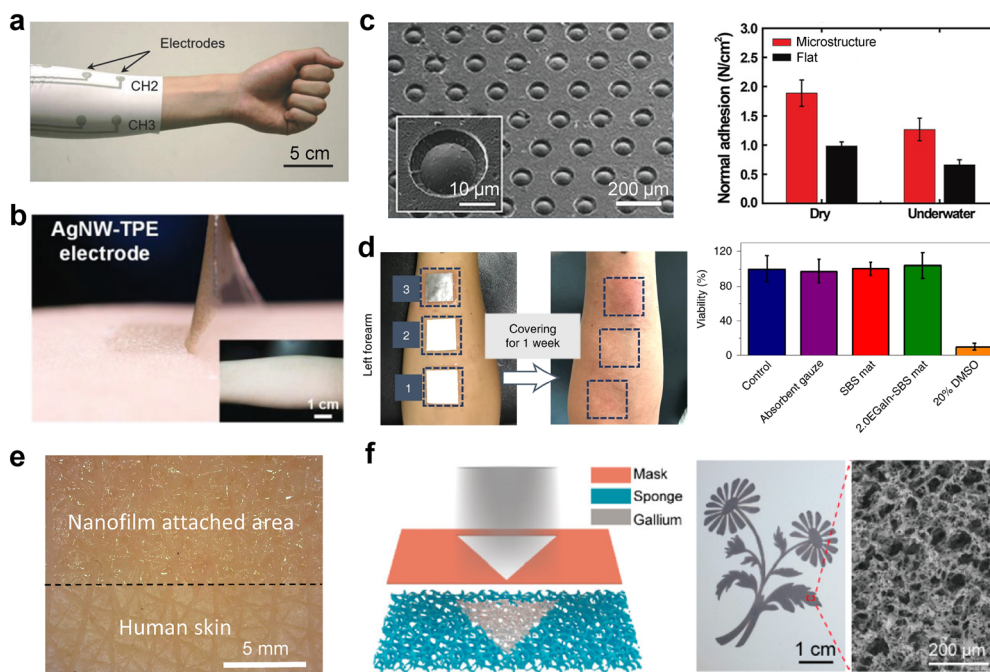


**Fig. 6** a) Optical Image showing a four-channel EMG system in the form of an armsleeve affixed to the body through mechanical compression. Reproduced with permission from ref. 69. Copyright 2017 John Wiley and Sons. b) Ultrathin Ag NW-based device on thermoplastic elastomer (TPE) film exhibiting firm attachment to the skin. Insets: Optical image showing the lack of any skin symptoms after device removal. Reproduced with permission from ref. 97. Copyright 2020 John Wiley and Sons. c) SEM image of a flexible film with octopus-inspired microcraters (OP) – conductive polymer composite (CPC) film and flat CPC film in dry and underwater conditions on a skin replica with the preload of 2 N cm<sup>-2</sup> (right). The inset is a magnified SEM image of the octopus-inspired microcrater. Reproduced with permission from ref. 98. Copyright 2018 John Wiley and Sons. d) Optical images showing the results of skin irritation on the forearms of a volunteer with different materials (left) and quantification of L-929 cell viability in different incubation groups (right). Reproduced with permission from ref. 99. Copyright 2021 Springer Nature. e) Optical image of nanofilm applied to the back of a hand. Reproduced with permission from ref. 100. Copyright 2021 Proceedings of the National Academy of Sciences. f) Schematic illustration of the liquid metal micromesh prepared by physically depositing liquid metal on the sponge. Optical and SEM images showing a representative flower-shaped pattern of the liquid metal micromesh. Reproduced with permission from ref. 101. Copyright 2022 American Chemical Society.





a robotic arm could be wirelessly controlled by the flexible sensing platform (Fig. 5g).

## 7. Desired attributes

In the realm of body-comfortable electronics, it is essential to consider both device functionalities and physiological comfort during device designs. This section will delve into the critical properties of adhesion, biocompatibility, and permeability.

### 7.1 Adhesion

The reliable adhesion of body-worn electronic devices is crucial for obtaining high-quality bio-signals.<sup>96</sup> Current research predominantly focuses on devices constructed on elastomer substrates, which inherently lack adhesion to the skin. Consequently, additional designs are required to ensure secure integration with the body. An effective way to achieve skin adhesion involves utilizing external forces through skin-tight compression garments. Jin *et al.* formulated a composite ink that can be directly screen printed into conductive features on regular textiles,<sup>69</sup> as depicted in Fig. 6a. An EMG monitoring system was prepared consisting of multiple biopotential sensors on a skin-tight arm sleeve, enabling the reliable acquisition of high-quality signals due to the tight fit based on compression forces.

An alternative method to achieve skin adhesion involves reducing the thickness of the device.<sup>102</sup> In the thin limit, the improved affinity of these devices to the skin is achieved through their conformal coverage on the textured surfaces due to the significantly decreased flexural rigidity. Nanofilms or nanomeshes in a few nanometers have demonstrated strong adhesion to the human skin.<sup>13,97,103</sup> In Fig. 6b, Yang *et al.* created a 150 nm-thick epidermal device on a thermoplastic elastomer substrate using a bubble-blowing process.<sup>97</sup> The peel strength of this ultrathin device from the skin is determined as 216 mN cm<sup>-1</sup>, indicating its capability to reliably adhere to the human body.

Another approach utilizes biocompatible adhesives or tapes to affix to the skin.<sup>99,104–106</sup> However, there is often a compromise between permeability and adhesion in these devices. While thick adhesives generally offer strong adhesion, they often have limited permeability. To tackle this issue, permeable sensors have been devised by creating through-hole patterns using lasers.<sup>107,108</sup> A specialized category of engineered dry adhesives employs tailored microstructures to improve adhesion based on physical mechanisms.<sup>98,109</sup> Chun *et al.* developed octopus-inspired microcraters with protuberances to augment skin adhesion (Fig. 6c).<sup>98</sup> This microstructured adhesive has a peel strength of 1.8 N cm<sup>-2</sup> for the dry state and 1.2 N cm<sup>-2</sup> for underwater conditions (Fig. 6c). The capability of wet adhesion surpasses numerous commercial adhesives.

### 7.2 Biocompatibility

The development of body-comfortable electronics with high biocompatibility has been a research focus, aiming to facilitate prolonged wear without inducing skin allergies or irritations. Biomass-based materials, including silk protein, gelatin, cellulose, chitin, and alginate, represent promising candidates for biocompatible substrates.<sup>64,110,111</sup> Conductive polymers, such as polypyrrole (PPy) and PEDOT:PSS, are considered benign components for creating functional electrodes and electrical interconnects.<sup>64,112</sup> Li *et al.* successfully integrated PEDOT:PSS into glycerol-plasticized silk fiber mats, demonstrating exceptional skin conformality and long-term compatibility.<sup>64</sup> These electrodes were employed for continuous ECG monitoring in various situations, including calm and post-exercise states. Furthermore, carbon-based nanomaterials like carbon nanotube (CNT) and graphene have been incorporated into these devices. For instance, a biocompatible and multifunctional patch was developed by dispersing highly conductive CNTs into biodegradable silk nanofibers, allowing for biopotential signal recording and drug delivery.<sup>113</sup> Gold, a biocompatible noble metal, has also been extensively utilized in this context.<sup>114</sup> The skin's reactions can be used to assess the compatibility of body-comfortable electronics. Ma *et al.* created biopotential sensors based on a liquid metal of EGaIn on electrospun SBS mats.<sup>99</sup> These sensors did not elicit any adverse reactions on the skin even after long-term attachments (Fig. 6d). Interestingly, *in vitro* tests were also performed by culturing cells together with the targeted materials (Fig. 6d). The high cell viability of SBS mats and liquid metal-based sensors further confirms their excellent biocompatibility at the cellular level.

### 7.3 Permeability

A crucial role of healthy human skin is to regulate the balance of heat and moisture. Stretchable electronic devices are predominantly constructed on elastomer substrates. While elastomers are generally nonideal barriers for gas molecules, the sub-millimeter substrates commonly adopted in the literature are sufficiently thick to impede gas diffusion.<sup>115,116</sup> Prolonged adherence of impermeable electronics to the skin can lead to discomfort and potentially adverse reactions.<sup>99,117</sup> When perspiration is unable to efficiently dissipate from the skin, it leads to the accumulation of moisture on the skin surface, causing unpleasant sensations such as dampness and clamminess. The buildup of sweat at the device-skin interface may diminish detection sensitivity. In this context, we will deliberate on several essential methods to achieve high permeability in body-worn devices.

**7.3.1 Ultrathin solid membrane.** An effective design uses ultrathin membranes of elastomers to build functional devices. Due to their rich free volume, elastomers serve as non-ideal barriers for gas molecules, providing substantially enhanced permeability in their ultrathin forms.<sup>116,118</sup> Wang



*et al.* successfully produced durable, self-adhesive, permeable nanofilms with an ultrathin thickness of 95 nm using a straightforward dip-coating technique (Fig. 6e).<sup>100</sup> The primary innovation lies in the ultrathin PDMS nanofilms on PU nanofibers, which exhibit enhanced robustness and exceptional permeability. The Au-coated nanofilms function as biopotential sensors capable of stable operation for up to 1 week, offering excellent skin conformability and a high SNR of 34 dB.

**7.3.2 Porous scaffold.** Porous scaffolds offer an alternative platform for the development of breathable devices. These scaffolds can be categorized into textiles and sponges based on their microstructures. Textiles adopt woven and non-woven designs,<sup>59,119</sup> whereas sponge substrates are formed using solid templates,<sup>101,120</sup> phase separation,<sup>121</sup> and breath figure methods.<sup>122</sup> The interconnected micropores within these porous substrates are crucial for superior permeability, providing extensive pathways for gas transport.<sup>123</sup> This porous design also helps to reduce mechanical stiffness. Various techniques have been developed to incorporate conductive materials into porous substrates, such as spray coating,<sup>124</sup> vacuum deposition,<sup>125</sup> and chemical deposition.<sup>126</sup> Porous scaffolds not only offer mechanical support but also provide a substrate for assembling conductive materials into interconnected networks. For example, several studies have explored the optimal methods for the assembly of Ag NWs on non-woven textiles to create breathable and stretchable conductors, which are used to develop functional sensors.<sup>117,127</sup> Additionally, conductive micromeshes made of liquid metals have been created on sponge substrates, combining excellent permeability and deformability (Fig. 6f).<sup>101</sup>

## 8. Conclusions and outlook

This article overviews recent progress in developing stretchable and body-conformable physical sensors. Wearable physical sensors have garnered significant attention due to their wide-ranging implications for healthcare. Stretchability and body conformability are crucial properties for these sensors to adapt to the body's contours, establishing robust interfaces for detecting various signals such as biopotential, hydration, temperature, and pressure. Moreover, recent advancements aimed at introducing new attributes into these systems, including adhesion, biocompatibility, and permeability, can potentially enhance the reliability and wearing comfort of these devices. Despite significant progress, there are ongoing challenges in various aspects that necessitate further development.

In the realm of wearable technology, the ability of devices to endure repetitive deformations significantly influences their reliability and long-term functionality. Practical concerns arise from delamination and cracks in the active layers of stretchable and wearable sensors, leading to drifted responses and potential failure. Employing self-healing

mechanisms inspired by biological processes offers a promising approach to repairing damaged materials and extending the lifespan of sensing devices. Recent studies have showcased the exceptional electromechanical durability of repairing damaged solid metal conductors using liquid metal microcapsules, indicating the need for further exploration in this domain.<sup>75,128</sup>

The successful commercialization of stretchable and body-conformable sensors necessitates cost-effective manufacturing and packaging methods. While micro-electro-mechanical systems technology has some cost barriers and is only compatible with limited types of devices, emerging printing technologies have the potential to reduce manufacturing costs through scalable production.<sup>129</sup> The printing equipment is more adaptable to new materials and their integration without significant alterations to the production line. Since most reported devices are prepared in lab settings, it is essential to identify low-cost manufacturing techniques for the successful translation of these promising sensing devices.

One of the most pressing challenges in current sensing systems is the reliance on rigid chips in signal processing circuits. This hybrid system can lead to undesired stress and hot spots when in contact with the skin.<sup>130–132</sup> To overcome these practical issues, it is vital to prioritize the integration of sensors and processing chips into the design considerations, creating stretchable and body-conformable devices at the system level. Moreover, adopting circuit architectures with robust noise immunity can facilitate the construction of complex circuits with signal conditioning capability. These efforts may lead to a fully stretchable sensing system with continuous, multifunctional healthcare or diagnostic capabilities, making a substantial breakthrough in practical clinical and medical applications.

A prevalent issue pertains to the power supply within the system, which should take a flexible and stretchable format. Energy harvesting devices that gain power from the surrounding environment are crucial to obviate the need for frequent recharging or battery replacement. Despite considerable efforts in developing deformable forms of power sources, further advancements are warranted. For instance, power sources such as supercapacitors and batteries should incorporate regulation circuits that align with the operation voltage window of the systems.<sup>133</sup> Intermittent power sources, such as piezoelectric/triboelectric generators and solar cells, should be coupled with energy storage devices to support the continuous operation of the sensing system.<sup>134</sup>

Despite these challenges and opportunities, stretchable and body-conformable physical sensors have great potential for fitness tracking, medical diagnosis, and human-machine interactions. These devices could be a game-changer for next-generation wearable technology. Collaboration between academia and industry is essential to transforming many exciting developments into useful gadgets and solutions.



## Data availability

Data available on request from the authors. The data that support the findings of this study are available from the corresponding author [Desheng Kong], upon reasonable request.

## Author contributions

The manuscript was written through contributions of all authors. All authors have approved the final version of the manuscript. Yong Lin: investigation, data collection, writing – original draft, writing – review & editing. Weijie Qiu: investigation, data collection. Desheng Kong: supervision, writing – review & editing, funding acquisition.

## Conflicts of interest

The authors declare no conflict of interest.

## Acknowledgements

We acknowledge the support from the National Natural Science Foundation of China (grant no. 62374083).

## References

- 1 J. A. Rogers, T. Someya and Y. Huang, *Science*, 2010, **327**, 1603–1607.
- 2 S. Wang, J. Y. Oh, J. Xu, H. Tran and Z. Bao, *Acc. Chem. Res.*, 2018, **51**, 1033–1045.
- 3 S. Choi, H. Lee, R. Ghaffari, T. Hyeon and D.-H. Kim, *Adv. Mater.*, 2016, **28**, 4203–4218.
- 4 S. Choi, S. I. Han, D. Jung, H. J. Hwang, C. Lim, S. Bae, O. K. Park, C. M. Tschabrunn, M. Lee, S. Y. Bae, J. W. Yu, J. H. Ryu, S.-W. Lee, K. Park, P. M. Kang, W. B. Lee, R. Nezafat, T. Hyeon and D.-H. Kim, *Nat. Nanotechnol.*, 2018, **13**, 1048–1056.
- 5 J.-W. Jeong, W.-H. Yeo, A. Akhtar, J. J. S. Norton, Y.-J. Kwack, S. Li, S.-Y. Jung, Y. Su, W. Lee, J. Xia, H. Cheng, Y. Huang, W.-S. Choi, T. Bretl and J. A. Rogers, *Adv. Mater.*, 2013, **25**, 6839–6846.
- 6 J. C. Yang, J. Mun, S. Y. Kwon, S. Park, Z. Bao and S. Park, *Adv. Mater.*, 2019, **31**, 1904765.
- 7 C. Wang, K. He, J. Li and X. Chen, *SmartMat*, 2021, **2**, 252–262.
- 8 M. Amjadi, K.-U. Kyung, I. Park and M. Sitti, *Adv. Funct. Mater.*, 2016, **26**, 1678–1698.
- 9 S. Zhao, W. Ran, L. Wang and G. Shen, *J. Semicond.*, 2022, **43**, 082601.
- 10 M. Tsai, P. Su and C. Lu, *Sens. Actuators, B*, 2020, **324**, 128728.
- 11 S. Nasiri and M. R. Khosravani, *Sens. Actuators, A*, 2020, **312**, 112105.
- 12 Y. Luo, M. R. Abidian, J.-H. Ahn, D. Akinwande, A. M. Andrews, M. Antonietti, Z. Bao, M. Berggren, C. A. Berkey and C. J. Bettinger, *ACS Nano*, 2023, **17**, 5211–5295.
- 13 Y. Wang, S. Lee, T. Yokota, H. Wang, Z. Jiang, J. Wang, M. Koizumi and T. Someya, *Sci. Adv.*, 2020, **6**, eabb7043.
- 14 S. Sahu, K. Tripathy, M. Bhattacharjee and D. Chopra, *Chem. Commun.*, 2024, **60**, 4382–4394.
- 15 S. Liu, Y. Rao, H. Jang, P. Tan and N. Lu, *Matter*, 2022, **5**, 1104–1136.
- 16 Y. Liu, M. Pharr and G. A. Salvatore, *ACS Nano*, 2017, **11**, 9614–9635.
- 17 Z. Xue, H. Song, J. A. Rogers, Y. Zhang and Y. Huang, *Adv. Mater.*, 2020, **32**, 1902254.
- 18 Y. Gao, L. Yu, J. C. Yeo and C. T. Lim, *Adv. Mater.*, 2020, **32**, 1902133.
- 19 Y. Huang, H. Wu, L. Xiao, Y. Duan, H. Zhu, J. Bian, D. Ye and Z. Yin, *Mater. Horiz.*, 2019, **6**, 642–683.
- 20 J. Kim, A. S. Campbell, B. E. F. de Ávila and J. Wang, *Nat. Biotechnol.*, 2019, **37**, 389–406.
- 21 Y. Wang, H. Haick, S. Guo, C. Wang, S. Lee, T. Yokota and T. Someya, *Chem. Soc. Rev.*, 2022, **51**, 3759–3793.
- 22 Y. Yang and W. Gao, *Chem. Soc. Rev.*, 2019, **48**, 1465–1491.
- 23 M. L. Hammock, A. Chortos, B. C. K. Tee, J. B. H. Tok and Z. Bao, *Adv. Mater.*, 2013, **25**, 5997–6038.
- 24 J.-W. Jeong, W.-H. Yeo, A. Akhtar, J. J. Norton, Y.-J. Kwack, S. Li, S.-Y. Jung, Y. Su, W. Lee and J. Xia, *Adv. Mater.*, 2013, **25**, 6839–6846.
- 25 S. Kabiri Ameri, R. Ho, H. Jang, L. Tao, Y. Wang, L. Wang, D. M. Schnyer, D. Akinwande and N. Lu, *ACS Nano*, 2017, **11**, 7634–7641.
- 26 F. Ershad, A. Thukral, J. Yue, P. Comeaux, Y. Lu, H. Shim, K. Sim, N.-I. Kim, Z. Rao and R. Guevara, *Nat. Commun.*, 2020, **11**, 3823.
- 27 D.-H. Kim and J. A. Rogers, *Adv. Mater.*, 2008, **20**, 4887–4892.
- 28 D.-H. Kim, N. Lu, R. Ma, Y.-S. Kim, R.-H. Kim, S. Wang, J. Wu, S. M. Won, H. Tao and A. Islam, *Science*, 2011, **333**, 838–843.
- 29 A. Lamoureux, K. Lee, M. Shlian, S. R. Forrest and M. Shtein, *Nat. Commun.*, 2015, **6**, 8092.
- 30 D.-H. Kim, J.-H. Ahn, W. M. Choi, H.-S. Kim, T.-H. Kim, J. Song, Y. Y. Huang, Z. Liu, C. Lu and J. A. Rogers, *Science*, 2008, **320**, 507–511.
- 31 C. Yan, J. Wang, X. Wang, W. Kang, M. Cui, C. Y. Foo and P. S. Lee, *Adv. Mater.*, 2014, **26**, 943.
- 32 J. Liang, L. Li, K. Tong, Z. Ren, W. Hu, X. Niu, Y. Chen and Q. Pei, *ACS Nano*, 2014, **8**, 1590–1600.
- 33 J. Y. Oh, S. Rondeau-Gagné, Y.-C. Chiu, A. Chortos, F. Lissel, G.-J. N. Wang, B. C. Schroeder, T. Kurosawa, J. Lopez, T. Katsumata, J. Xu, C. Zhu, X. Gu, W.-G. Bae, Y. Kim, L. Jin, J. W. Chung, J. B.-H. Tok and Z. Bao, *Nature*, 2016, **539**, 411.
- 34 Y. Kim, J. Zhu, B. Yeom, M. Di Prima, X. Su, J.-G. Kim, S. J. Yoo, C. Uher and N. A. Kotov, *Nature*, 2013, **500**, 59–63.
- 35 F. Xu and Y. Zhu, *Adv. Mater.*, 2012, **24**, 5117–5122.
- 36 J. Liang, L. Li, X. Niu, Z. Yu and Q. Pei, *Nat. Photonics*, 2013, **7**, 817–824.





- 37 W. Guo, P. Zheng, X. Huang, H. Zhuo, Y. Wu, Z. Yin, Z. Li and H. Wu, *ACS Appl. Mater. Interfaces*, 2019, **11**, 8567–8575.
- 38 C. Ding, J. Wang, W. Yuan, X. Zhou, Y. Lin, G. Zhu, J. Li, T. Zhong, W. Su and Z. Cui, *ACS Appl. Mater. Interfaces*, 2022, **14**, 29144–29155.
- 39 N. Matsuhisa, D. Inoue, P. Zalar, H. Jin, Y. Matsuba, A. Itoh, T. Yokota, D. Hashizume and T. Someya, *Nat. Mater.*, 2017, **16**, 834–840.
- 40 T. Nezakati, A. Seifalian, A. Tan and A. M. Seifalian, *Chem. Rev.*, 2018, **118**, 6766–6843.
- 41 C. Lim, Y. J. Hong, J. Jung, Y. Shin, S.-H. Sunwoo, S. Baik, O. K. Park, S. H. Choi, T. Hyeon and J. H. Kim, *Sci. Adv.*, 2021, **7**, eabd3716.
- 42 Q. Wang, Y. Li, Y. Lin, Y. Sun, C. Bai, H. Guo, T. Fang, G. Hu, Y. Lu and D. Kong, *Nano-Micro Lett.*, 2024, **16**, 87.
- 43 S. Chen, H.-Z. Wang, R.-Q. Zhao, W. Rao and J. Liu, *Matter*, 2020, **2**, 1446–1480.
- 44 J. Ma, F. Krisnadi, M. H. Vong, M. Kong, O. M. Awartani and M. D. Dickey, *Adv. Mater.*, 2023, **35**, 2205196.
- 45 G. Hu, H. Zhu, H. Guo, S. Wang, Y. Sun, J. Zhang, Y. Lin and D. Kong, *ACS Appl. Mater. Interfaces*, 2023, **15**, 28675–28683.
- 46 M. Shin, J. Y. Oh, K.-E. Byun, Y.-J. Lee, B. Kim, H.-K. Baik, J.-J. Park and U. Jeong, *Adv. Mater.*, 2015, **27**, 1255–1261.
- 47 E. Song, B. Kang, H. H. Choi, D. H. Sin, H. Lee, W. H. Lee and K. Cho, *Adv. Electron. Mater.*, 2016, **2**, 1500250.
- 48 Y. Zhou, S. Cao, J. Wang, H. Zhu, J. Wang, S. Yang, X. Wang and D. Kong, *ACS Appl. Mater. Interfaces*, 2018, **10**, 44760–44767.
- 49 H. Guo, Y. Lin, S. Gu, G. Hu, Q. Wang, C. Bai, Y. Sun, C. Yang, T. Fang, X. Chen, D. Li and D. Kong, *Nano Lett.*, 2024, **24**, 5904–5912.
- 50 F. Stauffer and K. Tybrandt, *Adv. Mater.*, 2016, **28**, 7200–7203.
- 51 H. Lee, T. K. Choi, Y. B. Lee, H. R. Cho, R. Ghaffari, L. Wang, H. J. Choi, T. D. Chung, N. Lu, T. Hyeon, S. H. Choi and D. H. Kim, *Nat. Nanotechnol.*, 2016, **11**, 566–572.
- 52 B. Xu, A. Akhtar, Y. Liu, H. Chen, W.-H. Yeo, S. I. Park, B. Boyce, H. Kim, J. Yu, H.-Y. Lai, S. Jung, Y. Zhou, J. Kim, S. Cho, Y. Huang, T. Bretl and J. A. Rogers, *Adv. Mater.*, 2016, **28**, 4462–4471.
- 53 T. Yokota, P. Zalar, M. Kaltenbrunner, H. Jinno, N. Matsuhisa, H. Kitanosako, Y. Tachibana, W. Yukita, M. Koizumi and T. Someya, *Sci. Adv.*, 2016, **2**, e1501856.
- 54 Z. Zhu, R. Li and T. Pan, *Adv. Mater.*, 2018, **30**, 1705122.
- 55 C. Wang, X. Li, H. Hu, L. Zhang, Z. Huang, M. Lin, Z. Zhang, Z. Yin, B. Huang, H. Gong, S. Bhaskaran, Y. Gu, M. Makihata, Y. Guo, Y. Lei, Y. Chen, C. Wang, Y. Li, T. Zhang, Z. Chen, A. P. Pisano, L. Zhang, Q. Zhou and S. Xu, *Nat. Biomed. Eng.*, 2018, **2**, 687–695.
- 56 Y. Kim, J. Suh, J. Shin, Y. Liu, H. Yeon, K. Qiao, H. Kum, C. Kim, H. Lee, C. Choi, H. Kim, D. Lee, J. Lee, J. Kang, B. Park, S. Kang, J. Kim, S. Kim, J. Perozek, K. Wang, Y. Park, K. Kishen, L. Kong, T. Palacios, J. Park, M. Park, H. Kim, Y. Lee, K. Lee, S. Bae, W. Kong, J. Han and J. Kim, *Science*, 2022, **377**, 859–864.
- 57 M. Zhu, H. Wang, S. Li, X. Liang, M. Zhang, X. Dai and Y. Zhang, *Adv. Healthcare Mater.*, 2021, **10**, 2100646.
- 58 H. Wu, G. Yang, K. Zhu, S. Liu, W. Guo, Z. Jiang and Z. Li, *Adv. Sci.*, 2021, **8**, 2001938.
- 59 X. Ma, M. Zhang, J. Zhang, S. Wang, S. Cao, Y. Li, G. Hu and D. Kong, *ACS Mater. Lett.*, 2022, **4**, 634–641.
- 60 E. Huigen, A. Peper and C. Grimbergen, *Med. Biol. Eng. Comput.*, 2002, **40**, 332–338.
- 61 Y. Zhao, S. Zhang, T. Yu, Y. Zhang, G. Ye, H. Cui, C. He, W. Jiang, Y. Zhai, C. Lu, X. Gu and N. Liu, *Nat. Commun.*, 2021, **12**, 4880.
- 62 S. Zheng, W. Li, Y. Ren, Z. Liu, X. Zou, Y. Hu, J. Guo, Z. Sun and F. Yan, *Adv. Mater.*, 2022, **34**, 2106570.
- 63 L. Ding, C. Hang, S. Yang, J. Qi, R. Dong, Y. Zhang, H. Sun and X. Jiang, *Nano Lett.*, 2022, **22**, 4482–4490.
- 64 Q. Li, G. Chen, Y. Cui, S. Ji, Z. Liu, C. Wan, Y. Liu, Y. Lu, C. Wang, N. Zhang, Y. Cheng, K.-Q. Zhang and X. Chen, *ACS Nano*, 2021, **15**, 9955–9966.
- 65 M. Sharifuzzaman, M. A. Zahed, S. Sharma, S. M. S. Rana, A. Chhetry, Y. D. Shin, M. Asaduzzaman, S. Zhang, S. Yoon, X. Hui, H. Yoon and J. Y. Park, *Adv. Funct. Mater.*, 2021, **32**, 2107969.
- 66 J. Xu, X. Li, H. Chang, B. Zhao, X. Tan, Y. Yang, H. Tian, S. Zhang and T.-L. Ren, *ACS Nano*, 2022, **16**, 6687–6699.
- 67 J. Dong, X. Tang, Y. Peng, C. Fan, L. Li, C. Zhang, F. Lai, G. He, P. Ma, Z. Wang, Q. Wei, X.-P. Yan, H.-L. Qian, Y. Huang and T. Liu, *Nano Energy*, 2023, **108**, 108194.
- 68 H. Zhao, Y. Zhou, S. Cao, Y. Wang, J. Zhang, S. Feng, J. Wang, D. Li and D. Kong, *ACS Mater. Lett.*, 2021, **3**, 912–920.
- 69 H. Jin, N. Matsuhisa, S. Lee, M. Abbas, T. Yokota and T. Someya, *Adv. Mater.*, 2017, **29**, 1605848.
- 70 S. P. Lacour, G. Courtine and J. Guck, *Nat. Rev. Mater.*, 2016, **1**, 1–14.
- 71 E. D. Pasmanasari and J. A. Pawitan, *Biomed. Pharmacol. J.*, 2021, **14**, 373–378.
- 72 H. Hallez, B. Vanrumste, R. Grech, J. Muscat, W. De Clercq, A. Vergult, Y. D'Asseler, K. P. Camilleri, S. G. Fabri, S. Van Huffel and I. Lemahieu, *J. Neuroeng. Rehabil.*, 2007, **4**, 46.
- 73 P. Won, J. J. Park, T. Lee, I. Ha, S. Han, M. Choi, J. Lee, S. Hong, K.-J. Cho and S. H. Ko, *Nano Lett.*, 2019, **19**, 6087–6096.
- 74 B. Xu, A. Akhtar, Y. Liu, H. Chen, W. H. Yeo, S. I. Park, B. Boyce, H. Kim, J. Yu, H. Y. Lai, S. Jung, Y. Zhou, J. Kim, S. Cho, Y. Huang, T. Bretl and J. A. Rogers, *Adv. Mater.*, 2016, **28**, 4462–4471.
- 75 Y. Lin, T. Fang, C. Bai, Y. Sun, C. Yang, G. Hu, H. Guo, W. Qiu, W. Huang, L. Wang, Z. Tao, Y. Q. Lu and D. Kong, *Nano Lett.*, 2023, **23**, 11174–11183.
- 76 X. Huang, H. Cheng, K. Chen, Y. Zhang, Y. Zhang, Y. Liu, C. Zhu, S. C. Ouyang, G. W. Kong, C. Yu, Y. Huang and J. A. Rogers, *IEEE Trans. Biomed. Eng.*, 2013, **60**, 2848–2857.
- 77 R. C. Webb, A. P. Bonifas, A. Behnaz, Y. Zhang, K. J. Yu, H. Cheng, M. Shi, Z. Bian, Z. Liu, Y.-S. Kim, W.-H. Yeo, J. S.



- Park, J. Song, Y. Li, Y. Huang, A. M. Gorbach and J. A. Rogers, *Nat. Mater.*, 2013, **12**, 938–944.
- 78 S. Lee, S. Franklin, F. A. Hassani, T. Yokota, M. O. G. Nayeem, Y. Wang, R. Leib, G. Cheng, D. W. Franklin and T. Someya, *Science*, 2020, **370**, 966–970.
- 79 J. H. Koo, S. Jeong, H. J. Shim, D. Son, J. Kim, D. C. Kim, S. Choi, J.-I. Hong and D.-H. Kim, *ACS Nano*, 2017, **11**, 10032–10041.
- 80 Z. Huang, Y. Hao, Y. Li, H. Hu, C. Wang, A. Nomoto, T. Pan, Y. Gu, Y. Chen, T. Zhang, W. Li, Y. Lei, N. Kim, C. Wang, L. Zhang, J. W. Ward, A. Maralani, X. Li, M. F. Durstock, A. Pisano, Y. Lin and S. Xu, *Nat. Electron.*, 2018, **1**, 473–480.
- 81 T. Q. Trung and N. E. Lee, *Adv. Mater.*, 2016, **28**, 4338–4372.
- 82 D.-Y. Youn, U. Jung, M. Naqi, S.-J. Choi, M.-G. Lee, S. Lee, H.-J. Park, I.-D. Kim and S. Kim, *ACS Appl. Mater. Interfaces*, 2018, **10**, 44678–44685.
- 83 S. Harada, K. Kanao, Y. Yamamoto, T. Arie, S. Akita and K. Takei, *ACS Nano*, 2014, **8**, 12851–12857.
- 84 N. T. Tien, S. Jeon, D. I. Kim, T. Q. Trung, M. Jang, B. U. Hwang, K. E. Byun, J. Bae, E. Lee and J. B. H. Tok, *Adv. Mater.*, 2014, **26**, 796–804.
- 85 M. Jung, K. Kim, B. Kim, H. Cheong, K. Shin, O.-S. Kwon, J.-J. Park and S. Jeon, *ACS Appl. Mater. Interfaces*, 2017, **9**, 26974–26982.
- 86 J. Yang, D. Wei, L. Tang, X. Song, W. Luo, J. Chu, T. Gao, H. Shi and C. Du, *RSC Adv.*, 2015, **5**, 25609–25615.
- 87 G. Y. Bae, J. T. Han, G. Lee, S. Lee, S. W. Kim, S. Park, J. Kwon, S. Jung and K. Cho, *Adv. Mater.*, 2018, **30**, 1803388–1803395.
- 88 C. Zhu, A. Chortos, Y. Wang, R. Pfattner, T. Lei, A. C. Hinckley, I. Pochorovski, X. Yan, J. W.-F. To, J. Y. Oh, J. B.-H. Tok, Z. Bao and B. Murmann, *Nat. Electron.*, 2018, **1**, 183–190.
- 89 C. Larson, B. Peele, S. Li, S. Robinson, M. Totaro, L. Beccai, B. Mazzolai and R. Shepherd, *Science*, 2016, **351**, 1071–1074.
- 90 J. Yang, S. Luo, X. Zhou, J. Li, J. Fu, W. Yang and D. Wei, *ACS Appl. Mater. Interfaces*, 2019, **11**, 14997–15006.
- 91 T. Li, H. Luo, L. Qin, X. Wang, Z. Xiong, H. Ding, Y. Gu, Z. Liu and T. Zhang, *Small*, 2016, **12**, 5042–5048.
- 92 W. Liu, N. Liu, Y. Yue, J. Rao, F. Cheng, J. Su, Z. Liu and Y. Gao, *Small*, 2018, **14**, e1704149.
- 93 N. Luo, W. Dai, C. Li, Z. Zhou, L. Lu, C. C. Poon, S. C. Chen, Y. Zhang and N. Zhao, *Adv. Funct. Mater.*, 2016, **26**, 1178–1187.
- 94 H. Xu, L. Gao, Y. Wang, K. Cao, X. Hu, L. Wang, M. Mu, M. Liu, H. Zhang, W. Wang and Y. Lu, *Nano-Micro Lett.*, 2020, **12**, 159.
- 95 G. Schwartz, B. C.-K. Tee, J. Mei, A. L. Appleton, D. H. Kim, H. Wang and Z. Bao, *Nat. Commun.*, 2013, **4**, 1859.
- 96 J.-W. Jeong, W.-H. Yeo, A. Akhtar, J. J. S. Norton, Y.-J. Kwack, S. Li, S.-Y. Jung, Y. Su, W. Lee, J. Xia, H. Cheng, Y. Huang, W.-S. Choi, T. Bretl and J. A. Rogers, *Adv. Mater.*, 2013, **25**, 6839.
- 97 X. Yang, L. Li, S. Wang, Q. Lu, Y. Bai, F. Sun, T. Li, Y. Li, Z. Wang, Y. Zhao, Y. Shi and T. Zhang, *Adv. Electron. Mater.*, 2020, **6**, 2000306.
- 98 S. Chun, D. W. Kim, S. Baik, H. J. Lee, J. H. Lee, S. H. Bhang and C. Pang, *Adv. Funct. Mater.*, 2018, **28**, 1805224.
- 99 Z. Ma, Q. Huang, Q. Xu, Q. Zhuang, X. Zhao, Y. Yang, H. Qiu, Z. Yang, C. Wang, Y. Chai and Z. Zheng, *Nat. Mater.*, 2021, **20**, 859–868.
- 100 Y. Wang, S. Lee, H. Wang, Z. Jiang, Y. Jimbo, C. Wang, B. Wang, J. J. Kim, M. Koizumi, T. Yokota and T. Someya, *Proc. Natl. Acad. Sci. U. S. A.*, 2021, **118**, e2111904118.
- 101 Y. Li, S. Wang, J. Zhang, X. Ma, S. Cao, Y. Sun, S. Feng, T. Fang and D. Kong, *ACS Appl. Mater. Interfaces*, 2022, **14**, 13713–13721.
- 102 K. Yamagishi, S. Takeoka and T. Fujie, *Biomater. Sci.*, 2019, **7**, 520–531.
- 103 Y. Wang, T. Yokota and T. Someya, *NPG Asia Mater.*, 2021, **13**, 22.
- 104 K.-I. Jang, S. Y. Han, S. Xu, K. E. Mathewson, Y. Zhang, J.-W. Jeong, G.-T. Kim, R. C. Webb, J. W. Lee, T. J. Dawidczyk, R. H. Kim, Y. M. Song, W.-H. Yeo, S. Kim, H. Cheng, S. I. Rhee, J. Chung, B. Kim, H. U. Chung, D. Lee, Y. Yang, M. Cho, J. G. Gaspar, R. Carbonari, M. Fabiani, G. Gratton, Y. Huang and J. A. Rogers, *Nat. Commun.*, 2014, **5**, 4779.
- 105 M. Lee, J. Kim, M. T. Khine, S. Kim and S. Gandla, *Nanomaterials*, 2023, **13**, 2467.
- 106 J. Kim, A. Banks, H. Cheng, Z. Xie, S. Xu, K.-I. Jang, J. W. Lee, Z. Liu, P. Gutruf, X. Huang, P. Wei, F. Liu, K. Li, M. Dalal, R. Ghaffari, X. Feng, Y. Huang, S. Gupta, U. Paik and J. A. Rogers, *Small*, 2015, **11**, 906.
- 107 Q. Tian, H. Zhao, R. Zhou, T. Li, J. Huang, W. Tong, R. Xie, Q. Li, G. Li and Z. Liu, *ACS Appl. Mater. Interfaces*, 2022, **14**, 52535–52543.
- 108 J. Zhang, M. Hu, X. Zheng, H. Wang, X. Li, X. Zhang and H. Yang, *Adv. Mater. Technol.*, 2023, **8**, 2300243.
- 109 H. Min, S. Jang, D. W. Kim, J. Kim, S. Baik, S. Chun and C. Pang, *ACS Appl. Mater. Interfaces*, 2020, **12**, 14425–14432.
- 110 L. W. Taylor, S. M. Williams, J. S. Yan, O. S. Dewey, F. Vitale and M. Pasquali, *Nano Lett.*, 2021, **21**, 7093–7099.
- 111 F. Chen, X. Li, G. Liu, J. Zhao, L. Zhao, Y. Shi, Y. Shi, Z. Xu, W. Guo and Y. Liu, *Adv. Mater. Technol.*, 2023, **8**, 2201980.
- 112 K. Zhang, N. Kang, B. Zhang, R. Xie, J. Zhu, B. Zou, Y. Liu, Y. Chen, W. Shi, W. Zhang, W. Huang, J. Wu and F. Huo, *Adv. Electron. Mater.*, 2020, **6**, 2000259.
- 113 N. Gogurla, Y. Kim, S. Cho, J. Kim and S. Kim, *Adv. Mater.*, 2021, **33**, 2008308.
- 114 Y.-T. Kwon, J. J. S. Norton, A. Cutrone, H.-R. Lim, S. Kwon, J. J. Choi, H. S. Kim, Y. C. Jang, J. R. Wolpaw and W.-H. Yeo, *Biosens. Bioelectron.*, 2020, **165**, 112404.
- 115 P. E. Cassidy, T. M. Aminabhavi and C. M. Thompson, *Rubber Chem. Technol.*, 1983, **56**, 594–618.
- 116 G. J. Van Amerongen, *J. Appl. Phys.*, 1946, **17**, 972–985.
- 117 Y. Wang, J. Wang, S. Cao and D. Kong, *J. Mater. Chem. C*, 2019, **7**, 9748–9755.



- 118 P. E. Cassidy, T. M. Aminabhavi and C. M. Thompson, Water permeation through elastomers and plastics, *Rubber Chem. Technol.*, 1983, **56**, 594–618.
- 119 A. Libanori, G. Chen, X. Zhao, Y. Zhou and J. Chen, *Nat. Electron.*, 2022, **5**, 142.
- 120 B. Sun, R. N. McCay, S. Goswami, Y. Xu, C. Zhang, Y. Ling, J. Lin and Z. Yan, *Adv. Mater.*, 2018, **30**, 1804327.
- 121 J. Park, Y. Lee, M. H. Barbee, S. Cho, S. Cho, R. Shanker, J. Kim, J. Myoung, M. P. Kim, C. Baig, S. L. Craig and H. Ko, *Adv. Mater.*, 2019, **31**, 1808148.
- 122 W. Zhou, S. Yao, H. Wang, Q. Du, Y. Ma and Y. Zhu, *ACS Nano*, 2020, **14**, 5798–5805.
- 123 M. S. Brown, M. Mendoza, P. Chavoshnejad, M. J. Razavi, G. J. Mahler and A. Koh, *Adv. Mater. Technol.*, 2020, **5**, 2000242.
- 124 Y. J. Fan, P. T. Yu, F. Liang, X. Li, H. Y. Li, L. Liu, J. W. Cao, X. J. Zhao, Z. L. Wang and G. Zhu, *Nanoscale*, 2020, **12**, 16053–16062.
- 125 S. Lee, D. Sasaki, D. Kim, M. Mori, T. Yokota, H. Lee, S. Park, K. Fukuda, M. Sekino, K. Matsuura, T. Shimizu and T. Someya, *Nat. Nanotechnol.*, 2019, **14**, 156.
- 126 Q. Zhuang, Z. Ma, Y. Gao, Y. Zhang, S. Wang, X. Lu, H. Hu, C. Cheung, Q. Huang and Z. Zheng, *Adv. Funct. Mater.*, 2021, **31**, 2105587.
- 127 Z. Jiang, M. O. G. Nayeem, K. Fukuda, S. Ding, H. Jin, T. Yokota, D. Inoue, D. Hashizume and T. Someya, *Adv. Mater.*, 2019, **31**, 1903446.
- 128 Y. Li, T. Fang, J. Zhang, H. Zhu, Y. Sun, S. Wang, Y. Lu and D. Kong, *Proc. Natl. Acad. Sci. U. S. A.*, 2023, **120**, e2300953120.
- 129 Z. Cui, *Sci. China: Technol. Sci.*, 2019, **62**, 224–232.
- 130 S. Yao, P. Ren, R. Song, Y. Liu, Q. Huang, J. Dong, B. T. O'Connor and Y. Zhu, *Adv. Mater.*, 2020, **32**, 1902343.
- 131 Y. Khan, M. Garg, Q. Gui, M. Schadt, A. Gaikwad, D. Han, N. A. Yamamoto, P. Hart, R. Welte and W. Wilson, *Adv. Funct. Mater.*, 2016, **26**, 8764–8775.
- 132 A. M. Hussain and M. M. Hussain, *Adv. Mater.*, 2016, **28**, 4219–4249.
- 133 C. Bai, S. Li, K. Ji, M. Wang and D. Kong, *Energy Mater.*, 2023, **3**, 300041.
- 134 T. R. Ray, J. Choi, A. J. Bandodkar, S. Krishnan, P. Gutruf, L. Tian, R. Ghaffari and J. A. Rogers, *Chem. Rev.*, 2019, **119**, 5461–5533.

